

Supplementary Materials for

Electric field control of magnetic domain wall motion via modulation of the Dzyaloshinskii-Moriya interaction

Tomohiro Koyama*, Yoshinobu Nakatani, Jun-ichi Ieda, Daichi Chiba*

*Corresponding author. Email: tkoyama@ap.t.u-tokyo.ac.jp (T.K.); dchiba@ap.t.u-tokyo.ac.jp (D.C.)

Published 21 December 2018, *Sci. Adv.* **4**, eaav0265 (2018)

DOI: 10.1126/sciadv.aav0265

This PDF file includes:

Section S1. EF effect on areal magnetic moment and anisotropy energy

Section S2. Numerical calculation of the saturation DW velocity

Fig. S1. Schematic illustration of the capacitor structure for the areal magnetization measurement.

Fig. S2. In-plane magnetization curves for the studied samples.

Fig. S3. Simulated DW velocities as a function of external magnetic field and the anisotropy and DMI dependences of the DW velocity.

Table S1. Summary of the capacitances for the capacitors.

Reference (31)

Section S1. EF effect on areal magnetic moment and anisotropy energy

The EF effect on the areal magnetic moment M_{st} was directly measured using a superconducting quantum interference device. M_s and t are the saturation magnetization and effective thickness of the total ferromagnetic layer of the present sample, respectively. Figure S1A shows the schematic image of the sample structure for the M_{st} measurement. The substrate with the Pt/Co/Pd layers was cut into a piece with an area of $3 \times 4 \text{ mm}^2$, and a capacitor structure was fabricated by forming a 50-nm-HfO₂ dielectric layer and a Cr / Au gate electrode. The gate electrode area, capacitance, and areal capacitance for the two samples with different t_{Co} are summarized in Table S1. The areal capacitances are $0.36 \sim 0.37 \text{ } \mu\text{F}/\text{cm}^2$, which is consistent with the expected value from the dielectric constant of HfO₂ (~ 20). In this measurement, V_G was limited within a range of $\pm 10 \text{ V}$ to prevent the dielectric breakdown. Figures S1B and C show the V_G dependences of M_{st} for the capacitors with the nominal Co thickness $t_{\text{Co}} = 0.78$ and 0.98 nm , respectively. In both samples, the V_G -induced change in M_{st} was very small. Assuming that M_{st} linearly changes with V_G , the modulation of M_{st} by $\pm 15 \text{ V}$ was expected to be below 1 %.

The areal perpendicular anisotropy energy $K_u t$ of our samples shown in Fig. 3 was obtained using a 30- μm -wide Hall bar sample with a 50-nm-thick HfO₂ layer and a gate electrode. The in-plane magnetic field $H_{//}$ dependence of the anomalous Hall resistance R_{Hall} was measured under V_G application, from which the normalized in-plane magnetization $m_{//}^n$ curve was reproduced (see fig.

S2A and B) (12). The saturation field $\mu_0 H_k$ and $K_u t$ were calculated using the following relations:

$$\mu_0 H_k = 2\mu_0 [H_{//} dm_{//}]^n \text{ and } K_u t = \mu_0 H_k M_s t / 2, \text{ respectively.}$$

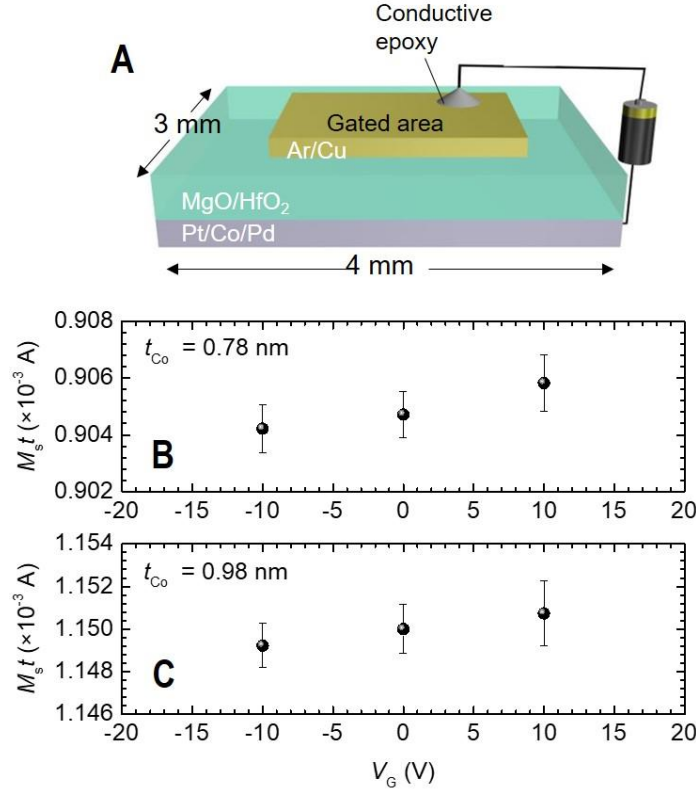


Fig. S1. Schematic illustration of the capacitor structure for the areal magnetization measurement. (A) Schematic illustration of the capacitor structure for the areal magnetization $M_s t$ measurement. A conductive epoxy was used for the electrical connection to the gate electrode. $M_s t$ as a function of gate voltage V_G for samples with Co thickness $t_{Co} =$ (B) 0.78 and (C) 0.98 nm. Each point is an average of 15 measurements, and the error bar is the standard deviation. The measurement was performed at 300 K.

Table S1. Summary of the capacitances for the capacitors.

t_{Co} (nm)	Gate electrode (mm ²)	Capacitance (nF)	Areal capacitance (μ F/cm ²)
0.78	2.2	8.1	0.37
0.98	1.8	6.5	0.36

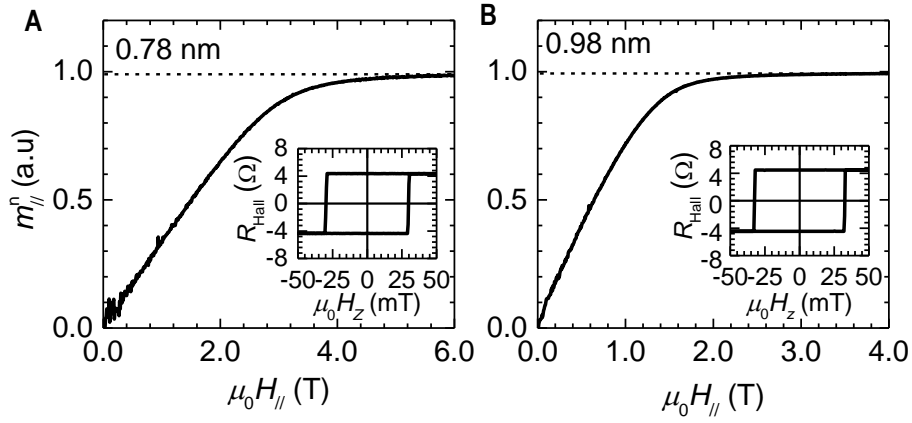


Fig. S2. In-plane magnetization curves for the studied samples. Normalized in-plane magnetization $m_{||}^n$ curves obtained by the anomalous Hall resistance R_{Hall} measurement for the samples with $t_{\text{Co}} =$ (a) 0.78 and (b) 0.98 nm at $V_G = 0$ V. The insets show the results of the R_{Hall} measurement with the perpendicular field $\mu_0 H_z$ sweep. The measurements were performed at 300 K.

From the V_G dependence of K_{ut} shown in Figs. 3A and B in the main text, the efficiencies of K_{ut} modulation by V_G for the $t_{\text{Co}} = 0.78$ and 0.98 nm samples were 120 and 20 fJ/Vm, respectively. The difference in the efficiency is most likely attributed to the difference in the electron structure of the top Pd layer between two samples. The built-in strain in the Pd layer depending on t_{Co} can be one possibility for this (31).

Section S2. Numerical calculation of the saturation DW velocity

We performed 2D micromagnetic simulations to investigate the effect of the EF-induced K_u and D change on the saturation DW velocity v_s . A 512-nm-wide wire with a single DW was used for the simulation. The mesh size was set to $2 \times 2 \times 0.98$ nm. A periodic boundary condition was applied in the direction of the wire width. To reproduce DW pinning, an anisotropy distribution was introduced to the system. Figure S3A shows the simulation results of v as a function of $\mu_0 H_z$ for $t_{Co} = 0.98$ nm. In this calculation, the experimentally determined values of M_s and K_u (1.17×10^5 A/m and 1.59×10^6 J/m³, respectively) were used. In addition, $A = 1.6 \times 10^{-11}$ J/m was assumed. Two different cases for D ($= 0$ and 0.5 mJ/m²) were calculated. The D value of 0.5 mJ/m² was determined from the areal DMI magnitude Dt obtained in the experiment (0.49 pJ/m) and the thickness of the Co layer (0.98 nm). As shown in fig. S3A, the v for $D = 0.5$ mJ/m² is higher than that for $D = 0$, and the saturation of v is reproduced only in the $D = 0.5$ mJ/m² case. This situation well reproduces the experimental result. A quantitative difference is probably because the parameter used in this simulation such as the exchange stiffness A differs from the actual value of our Pt/Co/Pd system. Figures S3B and C show v as a function of K_u and D at $\mu_0 H_z = 200$ mT, respectively. The values of K_u change used here are the same with the V_G -induced K_u change in the experiment. The simulated result shows that v is almost independent of K_u . On the other hand, an 8 % variation in D , which is obtained in this experiment, results in a clear v modulation. These results show that the 2D micromagnetic simulation, which is closer to the actual situation, supports the validity of the 1D model.

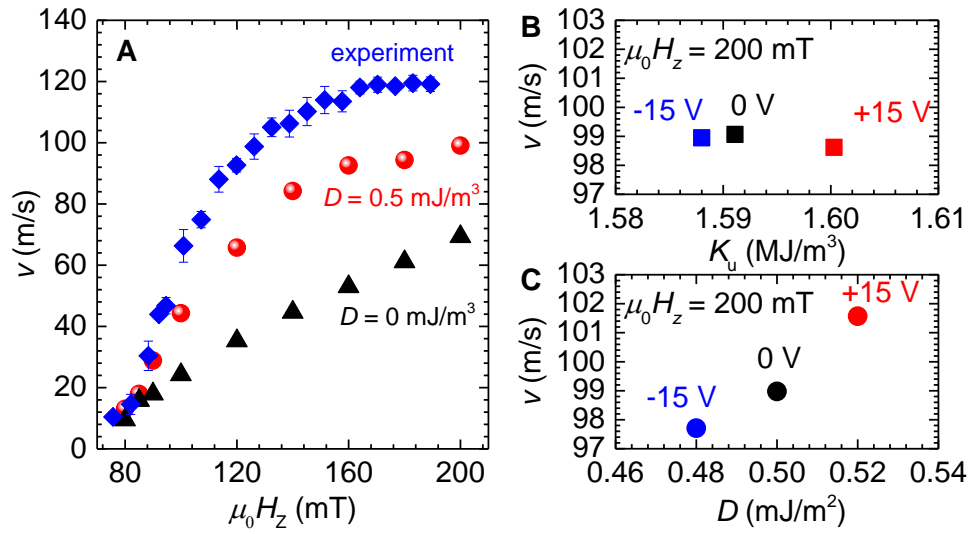


Fig. S3. Simulated DW velocities as a function of external magnetic field and the anisotropy and

DMI dependences of the DW velocity. (A) Simulated DW velocities (v) as a function of $\mu_0 H_z$ for the

DMI magnitude D of 0 (circle) and 0.5 mJ/m^2 (triangle). The experimentally-obtained v for $t_{co} = 0.98 \text{ nm}$

sample under $V_G = 0 \text{ V}$ is also plotted (diamond). v as a function of (B) K_u and (C) D calculated at $\mu_0 H_z = 200$

mT.